ISBN: 978-3-95450-248-6 ISSN: 2673-5490 doi: 10.18429/JACoW-IPAC2025-WEPS042

BENCHMARKING INTRABEAM SCATTERING WITH RF-TRACK

P. Desiré *[1], A. Latina, CERN, Geneva, Switzerland
S. Di Mitri[2], Elettra - Sincrotrone Trieste, Trieste, Italy
A. Gerbershagen, University of Groningen, Groningen, Netherlands
[1] also at University of Groningen, Groningen, Netherlands
[2] also at University of Trieste, Trieste, Italy

Abstract

Intra-beam scattering (IBS) has recently gained significant interest in the community of free electron lasers (FELs), as it is believed to produce an increment in the sliced energy spread (SES), which is detrimental to FEL performance.

To control and contain this phenomenon, it is important to include IBS in the design phase of an FEL through appropriate numerical simulation. Most existing codes that simulate IBS were developed for long-term tracking in circular lattices, assuming Gaussian bunches. Unfortunately, this assumption doesn't capture the rapid bunch evolution of electron bunches in photoinjectors. To address this limitation, the tracking code RF-Track has recently been updated to include IBS, using a novel hybrid-kinetic Monte Carlo method.

This paper presents benchmarks performed to verify the implementation. The predicted SES increment in the beam due to IBS using RF-Track has been compared against a kinetic approach used in a different tracking code and, secondly, against a semi-analytical model. The results showed a good agreement, setting RF-Track as a tool to understand and control the SES growth in photoinjectors and, in particular, in FELs.

INTRODUCTION

Intra-Beam Scattering (IBS), which refers to elastic Coulomb interactions within a beam, is a collective effect that can significantly impact the accelerator performance. IBS has been extensively studied in damping [1, 2] and storage rings [3].

Recent results indicate that IBS also affects linear accelerators, particularly free-electron laser light sources (FELs), where their high-brilliance, very dense beams are subjected to this effect. Studies have linked IBS with a Sliced-Energy Spread (SES) growth, potentially compromising the FEL performance. Measured SES values include 15 keV at SwissFEL with 200 pC bunches [4]), 6 keV at the European XFEL with 250 pC bunches [5] and 2 keV at PhotoInjector Test Facility at DESY Zeuthen with 250 pC bunches [6]. All of them are significantly higher than the about 1 keV predicted by simulations neglecting IBS.

FELs beams are highly non-Gaussian, making traditional IBS analytical models [7, 8] unsuitable. One can instead use Monte Carlo (MC) methods to fully integrate the actual shape of the phase space. Even though this comes at the cost of more computational time, it is still affordable in a one-pass machine like an FEL.

MC methods are implemented in tracking codes such as SIRE [9, 10] and MOCAC [11] for circular lattices. However, in an FEL, other effects, such as SC, wakefields, and non-linear fields in the electron gun, play an essential role. For this reason, RF-Track [12], a tracking code developed at CERN, which implements all the relevant effects for FEL beam dynamics, was recently extended to implement IBS using a hybrid MC method [13]. This paper presents a benchmarking of the simulation tool against numerical and analytical methods. Convergence tests validate the algorithm's robustness and stability.

METHOD

Update of the IBS Model

The hybrid-kinetic MC method implemented in RF-Track, previously detailed in [13], was recently modified to redefine the maximum impact parameter, $b_{\max}$. As the paper explains, this parameter is crucial for determining two key quantities: (1) the effective number of collisions via the total cross-section and (2) the Coulomb logarithm, which accounts for the long-range Coulomb interactions.

In RF-Track, $b_{\max}$ has been redefined to describe the boundary between short-range (collisional, IBS) and long-range (mean-field, Space Charge, SC) interactions, that is:

$$b_{\max} = \sqrt{h_x h_y / \pi}. \tag{1}$$

where h_x and h_y are the transverse mesh sizes of the 3D mesh used in the PIC space-charge calculation. This definition of $b_{\max}$ implies that SC and IBS are complementary and should always be used together, even though in the following, they are used individually for benchmarking reasons. The SC implementation in RF-Track was presented in [14].

SES Calculation

This work focuses on the effect of IBS on SES growth. However, the definition of SES varies among different studies. In these results, we measured the SES by subtracting the correlation in the longitudinal phase space using cubic spline interpolation. Then, we took the 10% of the particles closer to the median Z, in other words, the central longitudinal slide.

* pdesirev@cern.ch

ISBN: 978-3-95450-248-6 ISSN: 2673-5490 doi: 10.18429/JACoW-IPAC2025-WEPS042

RESULTS

Benchmark Against Another Numerical Approach

As a benchmark of the implementation, a test reproducing the studies of E. Gnojaj [15] has been performed. His work analyses the effect of IBS and SC for the European XFEL injector, starting after the gun and the harmonic modules, and studies the SES growth in a 19-m long drift. The same setup was simulated using RF-Track. The electron beam was characterized by the parameters in Table 1. The two codes used the same initial particle distribution. The results are shown in Fig. 1.

Table 1: Beam Characterization of the Particle Distribution Used in the Simulation Reproducing the European XFEL Injector [15]

Quantity	Value	Units
Bunch charge	250	pC
Kinetic energy	130	MeV
ϵ_{nx}, ϵ_{ny}	0.5464	mm·mrad
σ_x, σ_y	0.3168	mm
β_x, β_y	46.7	m
α_x, α_y	-2.04	
σ_z	1.2557	mm
σ_P/P	0.207	%

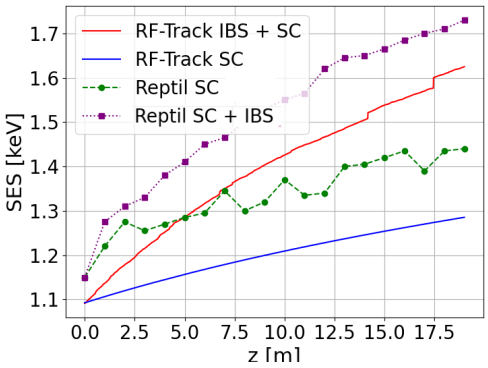

Figure 1: Comparison of the results of E. Gnojaj's code, Reptil [15], against RF-Track, in a 19m-long drift. The simulation includes SC effects and the combination of SC and IBS. The parameters replicate the conditions found at European XFEL and are described in Table 1.

Figure 1 shows the same SES growth due to IBS (≈ 0.31 keV) in the results of E. Gnojaj [15] and the ones of RF-Track, testifying to the good agreement between the two codes. An offset is observed between the pair of curves. This discrepancy arises from the different methods used to calculate the SES. The one used by E. Gnojaj was not completely described in his work, and it was not reproducible. A difference is evident even at the initial point, despite starting from the same distribution. The variation appears driven more by SC treatment than IBS. As discussed, both effects should ideally be considered together.

Benchmark Against a Semi-Analytical Model

The second benchmark has been performed with a semi-analytical method [16, 17] that provides the expected SES growth at the end of the drift due to IBS as well as to longitudinal SC. To count both effects together, the semi-analytical model adds their contributions quadratically. A 20m-long drift has been simulated under two sets of parameters, the low and the high charge cases, which have been described in Table 2. The SES growth along all the drift was analyzed with RF-Track for both cases, Fig. 2 shows the results obtained.

Table 2: Beam Characterization Used in the Low and High Charge Tests

Quantity	Low Charge	High Charge
Bunch charge (pC)	100	1000
Mean energy (MeV)	100	100
ϵ_{nx}, ϵ_{ny} (mm· mrad)	0.2	0.5
β_x, β_y (m)	20	20
α_x, α_y	1	1
σ_z (mm)	1.499	3.807
σ_E (keV)	1	1
Profile	Parabolic	Parabolic

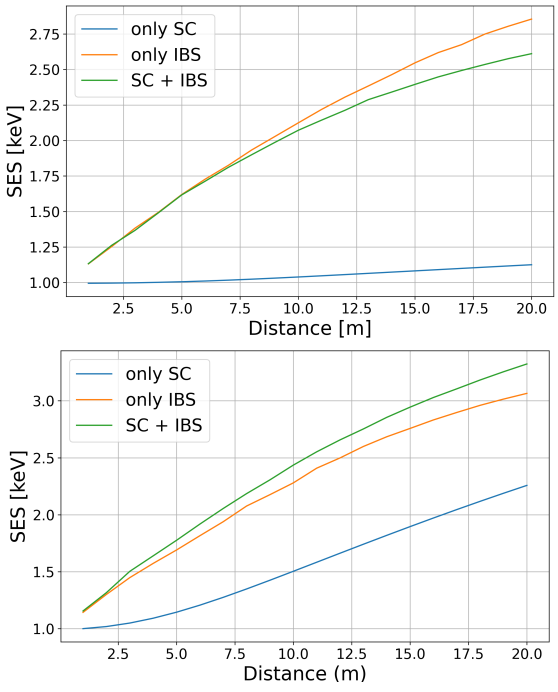

Figure 2: SES growth in the 20m-long drift due to SC (blue), IBS (yellow) and the combination of both (green) found by RF-Track. The top image corresponds to the low charge test whereas the bottom image corresponds to the high charge one. The beam initial conditions are reported in Table 2.

The SES predictions of the semi-analytical model have been reported in Table 3. Figure 2 shows that the final SES

ISBN: 978-3-95450-248-6 ISSN: 2673-5490 doi: 10.18429/JACoW-IPAC2025-WEPS042

Table 3: Final SES Computed by RF-Track Compared to the Semi-Analytical model (SA) in the Two Cases

Effect	Low Charge RF-Track	Low Charge SA	High Charge RF-Track	High Charge SA
Only SC (keV)	1.17	1.17	2.27	1.17
Only IBS (keV)	2.76	2.67	3.03	2.86
SC + IBS (keV)	2.52	2.74	3.28	2.94

values are similar to those computed semi-analytically and reported in Table 3 only in the IBS case. However, the SC predictions differ, especially in the high charge case. The difference is due to the simplified SC model assumed by the semi-analytical method, which implements the 1D Longitudinal SC impedance, 3D averaged over a transversely uniform cross-section, introduced in [18, 19].

Regarding the combined contribution of IBS and SC, the semi-analytical method quadratically adds the two separate contributions. On the other hand, RF-Track calculates the IBS and SC effects on each kick together, which generally does not lead to a quadratically addictive effect, and can even lead to a lower overall SES value such as the one observed in Fig. 2.

Convergence studies

The robustness of the proposed method has also been checked by changing the simulation setup, which depends on user-defined input parameters. First, the convergence of the algorithm was checked under different time steps. Second, since both IBS and SC algorithms share the same underlying 3D mesh (detailed on [12, 13]), a convergence study under the number of mesh points was also performed.

The same beam characterization of the high-charge test, described in Table 2, was used, as it had a larger IBS effect. The choice of lattice has been, again, a 20m-long drift. Figure 3 shows the SES found by RF-Track using different time steps. Figures 3 and 4 show the stability and robustness of the code by using different time steps and number of mesh points, establishing the algorithm as a reliable tool to measure SES at FELs.

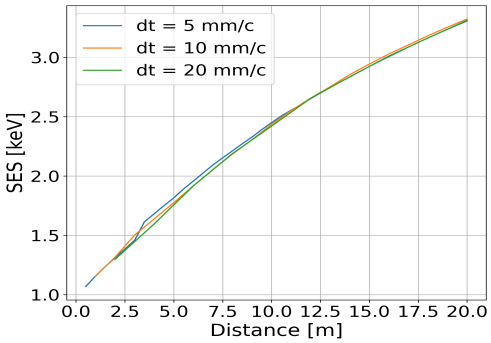

Figure 3: SES growth in the 20m-long drift due to SC and IBS together by RF-Track by using different time steps. The beam initial conditions were specified in Table 2.

Figure 4 shows RF-Track's values of the SES in the performed test with a different number of mesh points.

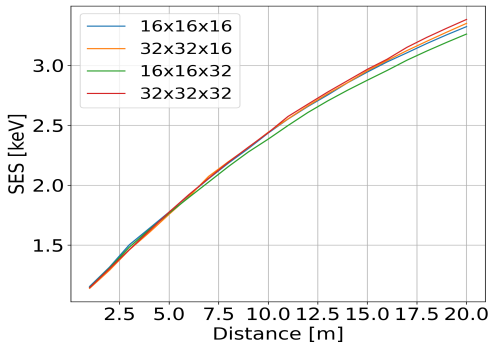

Figure 4: SES growth in the 20m-long drift with High-Charge configuration describe in Table 2 due to SC and IBS together by RF-Track by using different number of mesh points.

CONCLUSION

The IBS implementation of RF-Track has been benchmarked against a numerical method integrated into another tracking code, as well as a semi-analytical method developed by one of the authors. The benchmark against the numerical method further developed and implemented by one of the authors [16, 17] was performed on a 19m-long drift reproducing European XFEL's beam characteristics. An SES increment of 0.3 keV due to IBS was observed for both codes. The benchmark against the semi-analytical method was performed over a 20m-long drift using two different beam configurations. The two methods presented similar results regarding the IBS effect on the SES growth. The differences found in the results mainly came from the inclusion of the SC effects. Another source of discrepancy may be the methods used to calculate the SES, which vary widely in the literature and are often not specified.

Future steps for this work will include a benchmark with the semi-analytical model using a FODO lattice. Regarding the European XFEL simulation, it is proposed that the study be extended to do a benchmark against their experimental results. Furthermore, the simulations will be extended to a larger lattice like CERN's Proton Synchrotron Booster, where extensive literature documenting the impact of IBS exists. The expected effect of IBS is not only an increment of SES but also an increase in emittance growth. In that case, RFTrack results could be compared against one of the aforementioned codes for circular lattices. Finally, a benchmark against the experimental results found at SwissFEL is planned to fully understand the contribution of IBS to the observed SES growth.

ACKNOWLEDGEMENTS

The authors thank E. Gnojaj for providing the initial phase space coordinates and simulation data to benchmark against his results.

ISBN: 978-3-95450-248-6 ISSN: 2673-5490 doi: 10.18429/JACoW-IPAC2025-WEPS042

REFERENCES

[1] M. Zampetakis *et al.*, "Interplay of space charge, intra-beam scattering, and synchrotron radiation in the Compact Linear Collider damping rings", *Phys. Rev. Acc. Beams*, vol. 27, p. 064403, Jun. 2024. doi:10.1103/PhysRevAccelBeams.27.064403

[2] F. Antoniou, "Optics design of Intrabeam Scattering dominated damping rings", PhD Thesis, Univ. of Athens, Athens, Greece, 2012.

[3] S. Papadopoulou, "Bunch characteristics evolution for lepton and hadron rings under the influence of the Intra-beam scattering effect", PhD Thesis, Univ. of Crete, Crete, Greece, 2019.

[4] E. Prat *et al.*, "Energy spread blowup by intrabeam scattering and microbunching at the SwissFEL injector", *Phys. Rev. Accel. Beams*, vol. 25, p. 104401, Oct. 2022. doi:10.1103/PhysRevAccelBeams.25.104401

[5] S. Tomin *et al.*, "Accurate measurement of uncorrelated energy spread in electron beam", *Phys. Rev. Accel. Beams*, vol. 24, p. 064201, Jun. 2021. doi:10.1103/PhysRevAccelBeams.24.064201

[6] H. Qian *et al.*, "Slice energy spread measurement in the low energy photoinjector", *Phys. Rev. Accel. Beams*, vol. 25, p. 083401, Aug. 2022. doi:10.1103/PhysRevAccelBeams.25.083401

[7] A. Piwinski, "Excitation and damping of betratron oscillations and energy spread due to intra-beam scattering", in *Proc. 9th Int. Conf. Part. Accel.*, 1974.

[8] D. Bjorken, S.K. Mtingwa, "Intrabeam Scattering", *Part. Acc*, vol. 13, pp. 115–143, 1983.

[9] S. Papadopoulou *et al*., "Impact of non-Gaussian beam profiles in the performance of hadron colliders", *Phys. Rev. Accel. Beams*, vol. 23, p. 101004, Oct. 2020. doi:10.1103/PhysRevAccelBeams.23.101004

[10] A. Vivori, M. Martini, "Intra-beam scattering in the CLIC Damping Rings", in *Proc. IPAC'10*, Kyoto, Japan, May 2010, paper WEPE090, pp. 3557–3559.

[11] P. Zenkevich, O. Boine-Frankenheim, A. Bolshakov, "A new algorithm for the kinetic analysis of intra-beam scattering in storage rings", *Nucl. Instrum. Methods Phys. Res.*, vol. 561, pp. 284-288, 2006.

[12] A. Latina, "RF-Track reference manual", Jun. 2020, doi:10.5281/zenodo.4580369

[13] P. Desire Valdor, A. Gerbershagen, and A. Latina, "Intrabeam scattering simulation with a novel hybrid-kinetic Monte Carlo method for linear accelerators", in *Proc. LINAC'24*, Chicago, IL, USA, Aug. 2024, pp. 659–662. doi:10.18429/JACoW-LINAC2024-THPB014

[14] G. Bellodi, J. B. Lallement, A. Latina, A. M. Lombardi, "Benchmarking of PATH and RF-Track in the Simulation of Linac4", in *Proc. 68th Adv. Beam Dyn. Workshop High-Intensity High-Brightness Hadron Beams*, Geneva, Switzerland, Oct. 2023.

[15] E. Gjonaj, "Intrabeam Scattering effects in the electron injector of the European XFEL", in *Proc. FEL'22*, Trieste, Italy, Aug. 2022. doi:10.18429/JACoW-FEL2022-WEP14

[16] S. Di Mitri *et al.*, "Experimental evidence of intrabeam scattering in a free-electron laser driver", *New J. Phys.,* vol 22, p. 083053, Aug. 2019. doi:10.1088/1367-2630/aba572

[17] G. Perosa, S. Di Mitri, "Matrix model for collective phenomena in electron beam's longitudinal phase space", *Sci. Rep.,* vol 11, 7895, Aug. 2021. doi:10.1038/s41598-021-87041-0

[18] J. Rosenzweig *et al.*, "Space-charge oscillations in a self-modulated electron beam in multi-undulator free-electron lasers", *Nucl. Instr. and Meth. A*, vol 393, p. 376-379, Jul. 1997. doi:10.1016/S0168-9002(97)00516-0

[19] M. Venturini, "An effective longitudinal space-charge impedance model for beams with non-uniform and non-axis-symmetric transverse density", Rep. LBNL-63111, Berkeley, California, Jul. 2007.